Proceedings of DSCC2008
2008 ASME Dynamic Systems and Control Conference
October 20-22, 2008, Ann Arbor, Michigan, USA

DSCC2008-2183

VEHICLE DYNAMICS IN RESPONSE TO THE MANEUVER OF PRECISION IMMOBILIZATION TECHNIQUE

Jing Zhou
Dept. of Mechanical Engineering
University of Michigan
Ann Arbor, MI 48109
jzhouz@umich.edu

Jianbo Lu
Research & Advanced Engineering
Ford Motor Company
Dearborn, MI 48124
jlu10@ford.com

Huei Peng
Dept. of Mechanical Engineering
University of Michigan
Ann Arbor, MI 48109
hpeng@umich.edu

ABSTRACT

The Precision Immobilization Technique (PIT) is a maneuver frequently used by the law enforcement to terminate a hazardous vehicle pursuit situation. The maneuver is performed by intentionally nudging the pursued vehicle sideways to create large yaw motion which renders the pursued vehicle out of control. This work investigates the behavior of vehicles involved in this maneuver, develops dynamics models for the pre-impact, impact, and post-impact stages. Simulation results provide guidelines for the effective execution of the maneuver. In addition, the case for the vehicle equipped with an active yaw control system, such as the Electronic Stability Control, in response to the PIT maneuver is also addressed.

NOMENCLATURE

a, b	Distances from axles to vehicle CG
C_f, C_r	Cornering stiffness per axle, front and rear
D_s, K_s	Total suspension roll damping and roll stiffness
e	Coefficient of restitution in collisions
F_x, F_y	Components of the external impact force
F_{yf}, F_{yr}	Lateral tire forces per axle, front and rear
h	Distance from sprung mass CG to the roll axis
I_{xxs}	Sprung mass roll moment of inertia about roll axis
I_{xz}	Sprung mass product of inertia about roll & yaw axes
I_{zz}	Vehicle yaw moment of inertia about z axis
L	Wheelbase ($L = a + b$)
m_R, m_{NR}	Rolling mass, non-rolling mass
M	Total vehicle mass ($M = m_R + m_{NR}$)
P_x, P_y	Components of the external collision impulse
x_A, y_A, z_A	Coordinates of the impact location wrt vehicle CG
Δt	Duration of a collision
μ	Coefficient of tangential interaction in collisions
μ_R	Road adhesion coefficient

INTRODUCTION

Motor vehicle pursuit is one of high-risk activities for the law enforcement to undertake. Every year in the United States, hundreds of persons (including police officers, fleeing suspects, and innocent passers-by) are killed or injured during the course of pursuits [1]. Pursuit-related accidents, injuries and fatalities impose tremendous psychological stress on officers, and frequently result in negative public relations for police departments.

In an effort to reduce the risks inherent in motor vehicle pursuits, the Precision Immobilization Technique (PIT, also known as Pursuit Intervention Technique) [2], [3] is progressively used by the police to avert a prolonged vehicle chase in a safe manner. In a PIT maneuver, the police vehicle purposely strikes the fleeing vehicle at a certain location, which throws the vehicle into an abrupt spin, and puts a swift end to a high-speed pursuit (see Fig. 1, a screen capture from [4]).

The first law enforcement agency to employ PIT as a technique to halt pursued vehicles was the Fairfax County Police Department of Virginia in 1985 [5]. Executed properly in the right set of circumstances, the PIT is increasingly deemed a practical way to stop a fleeing vehicle when other tactics such as barricading, tire deflation or box-in are not feasible or ineffective. According to a 3-year California pursuit statistics [6], the majority of pursuits (79% of all) last shorter than 7 minutes, and 26% of all pursuits involve collisions. PIT maneuvers are often conducted against suspects who pose great risk to public safety.

The execution of PIT requires proper training, planning, choice of site, and careful timing. Under high stress, the police officers must not only choose the best tactics to put the pursued vehicle out of action, but also minimize its safety impact on the surrounding traffic, themselves, and even the suspect. In the court case Scott v. Harris [7], decided by the U.S. Supreme Court on April 30, 2007, it was ruled that “a police officer’s attempt to terminate a dangerous high-speed car chase that threatens the lives of innocent bystanders does not violate the Fourth Amendment, even when it places the fleeing motorist at risk of serious injury or death”. This court decision provides favorable judicial support for the law enforcement to use controlled contact (including PIT) against fleeing violators.

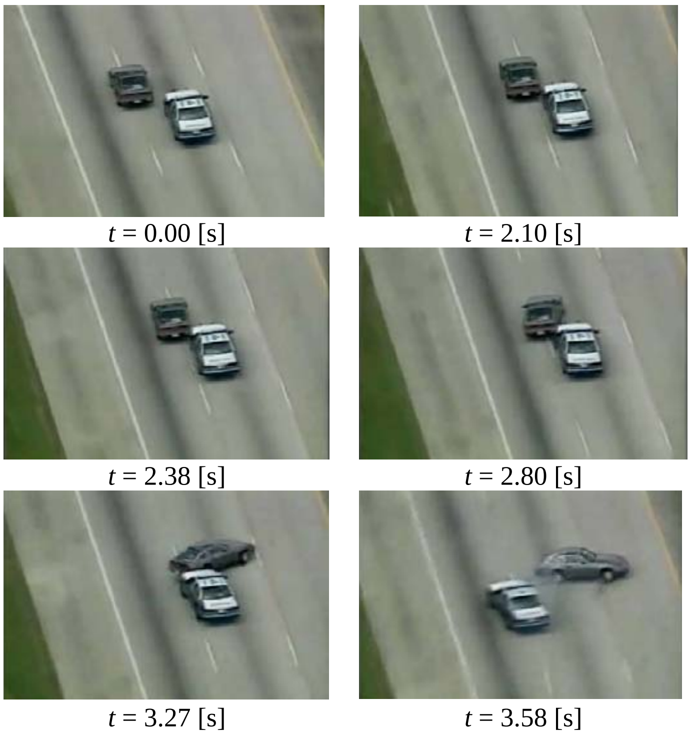

FIGURE 1. A PIT MANEUVER IN ACTION [4]

This work develops mathematical models for the vehicles involved in a PIT maneuver, provides guidelines for an effective PIT maneuver by employing a vehicle collision model, and investigates the control effectiveness of drivers’ counter-steering and active safety systems such as Electronic Stability Control (ESC). Because of the similarities between PIT collisions and some lane change/merge accidents, the analysis herein may also be applied to the study on vehicle collisions in this category.

GENERAL PROCEDURE OF A PIT MANEUVER

In a PIT maneuver (Fig. 2), the pursuing vehicle (pursuer) first pulls alongside with the pursued vehicle (target) from behind, so that the portion of the pursuing vehicle forward of the front axle is aligned with the portion of the pursued vehicle behind the rear axle. The pursuer first maintains a limited lateral clearance from the target's rear fender, and then steers sharply into the target. This sudden steering imparts an impulsive force to the pursued vehicle, and compels it to spin. After the initial collision, usually the pursuer keeps steering in the original direction and shoves the rear part of the target sideways, until the two vehicles separate and the pursued vehicle develops a heading angle too large to recover from.

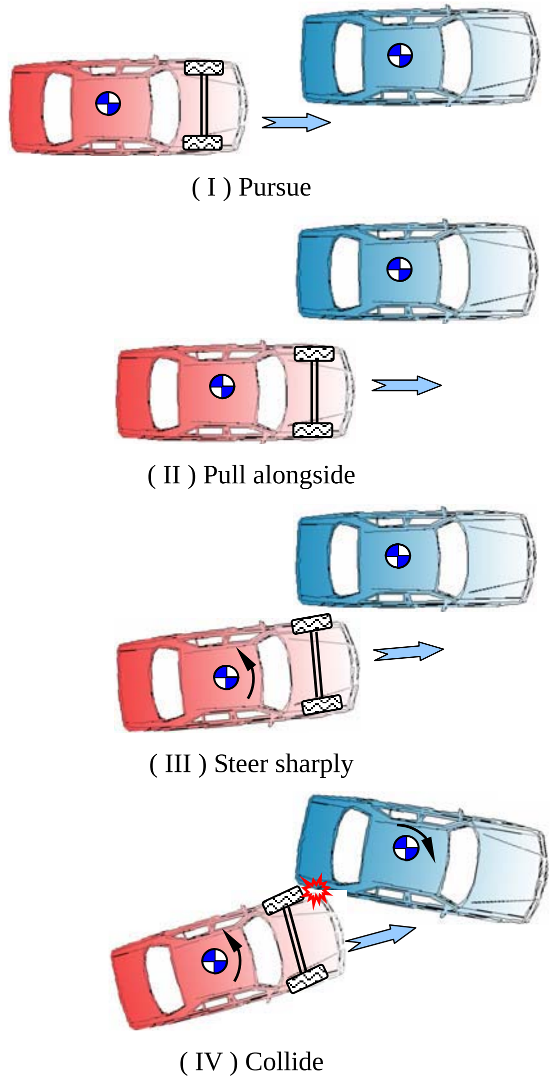

FIGURE 2. STAGES OF A PIT MANEUVER

The PIT maneuver is applicable only under certain situations. In view of the potential liabilities for the incurred injury or death, especially of bystanders and innocent drivers, many departments stipulate rules for the execution of PIT. Presently there is no uniform standard for the cut-off speed at which the use of PIT maneuver is disallowed. In some cases, the PIT is considered non-deadly force when properly executed at the maximum speed of 50 mph (80.5 km/h) [8]. Out of concerns over potential soil-tripped rollover accidents after the PIT maneuver, this cut-off speed is sometimes set lower, such as 45 mph (72.4 km/h). In addition, extra caution should be exercised when the two vehicles' bumpers are of significantly different heights, or if used against pursued vehicles with a high center of gravity, such as SUVs.

MODELING OF VEHICLE DYNAMICS IN A PIT MANEUVER

Pre-Impact Behavior of the Pursuing Vehicle

As illustrated in Fig. 2, the pursuing vehicle first adjusts its longitudinal position relative to the target vehicle, and maintains a lateral clearance before the impact. When the opportunity comes to initiate intervention maneuver, the pursuer steers sharply towards the target vehicle, develops a pre-impact yaw rate until the two vehicles collide.

Given road adhesion conditions and forward speed, the pursuer should properly adjust two operation variables to maximize the effect of collision: steering wheel angular velocity and initial lateral clearance. For simplicity, the steering action of the pursuer is modeled with a ramp input below, where the steering wheel turning rate is k_δ , and t = 0 denotes the instant of steering initiation.

$$\delta_{SW}(t) = k_\delta \cdot t \tag{1}$$

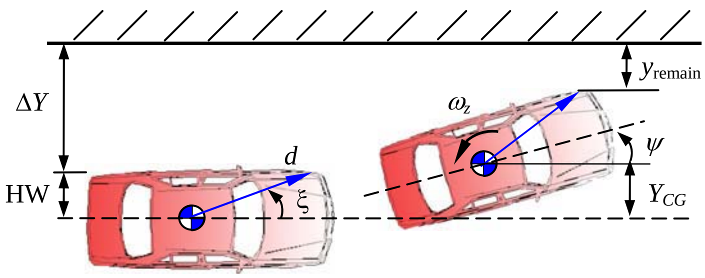

FIGURE 3. DETERMINATION OF THE COLLISION INSTANT

The initial lateral clearance (ΔY) affects the development of the pre-impact states of the pursuer. Given the vehicle's half-width (HW), the angle between vehicle centerline and the front fender (ξ), the lateral displacement (Y_{CG}), as well as the heading angle (ψ), their geometric relationship is depicted in Fig. 3, in which the struck side of the target vehicle is represented by a wall. Accordingly, the clearance between the pursuer and the target (y_{remain}) is given by

$$y_{\text{remain}} = \Delta Y + \text{HW} - Y_{CG} - d \sin(\psi + \xi) \tag{2}$$

Collision occurs at the instant when y_{remain} drops to zero. The vehicle dynamic responses to a steering input as in Equation (1) can be approximated by using a standard 2-DOF bicycle model, or computed from a nonlinear model of higher complexity, such as in the CarSim software.

Vehicle Collision Model during a PIT Maneuver

In order to characterize vehicle motions during the impact, a collision model is essential. This model should not only compute the collision forces generated within the short time span of contact, but also dictate the initial kinematic conditions for the ensuing motions after the impact. In this section, a previously developed model [9] for light impacts is applied to the PIT scenario. Unlike typical circumstances encountered in the studies on vehicle passive safety, usually no substantial structural deformation occurs in a PIT maneuver. Therefore, the focus of this model is on the characterization of vehicle kinematic motions after collisions, rather than on the analysis of vehicle crashworthiness or passenger injury.

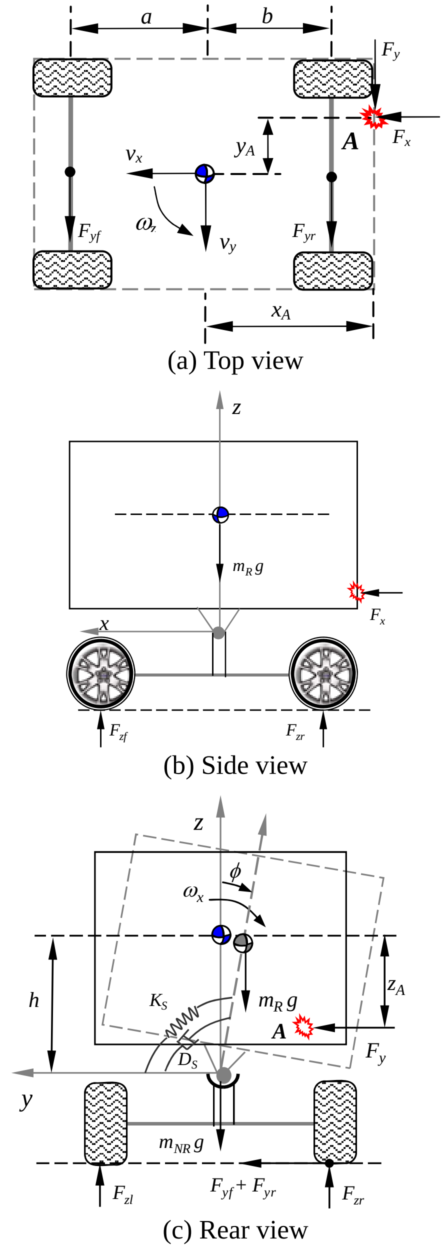

FIGURE 4. DIAGRAMS OF THE 4-DOF VEHICLE MODEL

The following paragraphs are a brief recount of the model development in [9]. The individual vehicle is treated as a 4-DOF lateral-yaw-roll model subject to external forces applied on the sprung mass (Fig. 4). The dynamic equations of motion in terms of longitudinal, lateral velocities, as well as rotational motion about the *x*-axis (roll) and the *z*-axis (yaw) are formulated as follows.

$$M(\dot{v}_x - v_y\omega_z) = F_x \tag{3}$$

$$M(\dot{v}_y + v_x\omega_z) - m_R h\dot{\omega}_x = F_y + F_{yf} + F_{yr} \tag{4}$$

$$I_{zz}\dot{\omega}_z + I_{xz}\dot{\omega}_x = x_A F_y - y_A F_x + aF_{yf} - bF_{yr} \tag{5}$$

$$\begin{aligned} I_{xxs}\dot{\omega}_x + I_{xz}\dot{\omega}_z - m_R h(\dot{v}_y + v_x\omega_z) = \\ F_y\left(z_A - h\right) + (m_R gh - K_s)\phi - D_s\omega_x \end{aligned} \tag{6}$$

where $\begin{cases} F_{yf} = C_f\left(\delta_f - \dfrac{v_y + a\omega_z}{v_x}\right), & \left|F_{yf}\right| < Mg\mu_R\dfrac{b}{L} \\ F_{yr} = C_r\left(\dfrac{-v_y + b\omega_z}{v_x}\right), & \left|F_{yr}\right| < Mg\mu_R\dfrac{a}{L} \end{cases}.$

A generic collision scenario is depicted in Fig. 5. Coordinates systems are defined as illustrated in the figure. A total of 12 unknowns need to be solved: post-impact longitudinal and lateral velocities, yaw and roll rates for both bullet and target vehicles (V_{1x}, V_{1y}, Ω_{1z}, Ω_{1x}, $V_{2x'}$, $V_{2y'}$, Ω_{2z}, $\Omega_{2x'}$), as well as the collision-induced impulses acting on the vehicles (P_x, P_y, $P_{x'}$, $P_{y'}$). The eight pre-impact vehicle states (v_{1x}, v_{1y}, ω_{1z}, ω_{1x}, $v_{2x'}$, $v_{2y'}$, ω_{2z}, $\omega_{2x'}$) are assumed to be available.

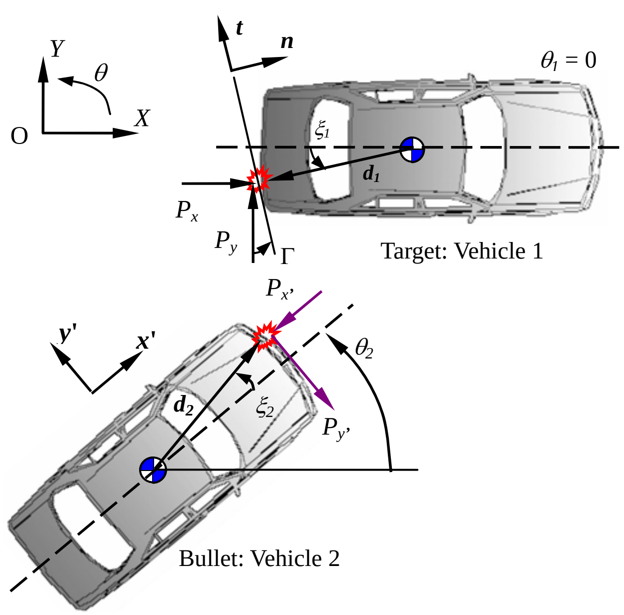

FIGURE 5. A GENERIC COLLISION SCENARIO

First integrate the above differential equations within the short duration of a collision. Equations (7) - (10) present the formulation for the target vehicle. The corresponding equations for the bullet vehicle can be obtained in the same way and are omitted here.

$$M_1 \cdot \left(V_{1x} - v_{1x}\right) - M_1\frac{\Delta t}{2}\left(V_{1y}\Omega_{1z} + v_{1y}\omega_{1z}\right) = P_x \tag{7}$$

$$\begin{aligned} M_1 \cdot \left(V_{1y} - v_{1y}\right) + M_1\frac{\Delta t}{2}\left(V_{1x}\Omega_{1z} + v_{1x}\omega_{1z}\right) - m_{R1}h_1 \cdot \left(\Omega_{1x} - \omega_{1x}\right) = \\ P_y - \frac{\Delta t}{2}C_{f1}\left(\frac{V_{1y} + a_1\Omega_{1z}}{V_{1x}} - \frac{v_{1y} + a_1\omega_{1z}}{v_{1x}}\right) - \frac{\Delta t}{2}C_{r1}\left(\frac{V_{1y} - b_1\Omega_{1z}}{V_{1x}} - \frac{v_{1y} - b_1\omega_{1z}}{v_{1x}}\right) \end{aligned} \tag{8}$$

$$\begin{aligned} I_{zz1}\left(\Omega_{1z} - \omega_{1z}\right) + I_{xz1}\left(\Omega_{1x} - \omega_{1x}\right) = P_y x_A - P_x y_A - \\ \frac{\Delta t}{2}a_1C_{f1}\left(\frac{V_{1y} + a_1\Omega_{1z}}{V_{1x}} - \frac{v_{1y} + a_1\omega_{1z}}{v_{1x}}\right) + \frac{\Delta t}{2}b_1C_{r1}\left(\frac{V_{1y} - b_1\Omega_{1z}}{V_{1x}} - \frac{v_{1y} - b_1\omega_{1z}}{v_{1x}}\right) \end{aligned} \tag{9}$$

$$\begin{aligned} I_{xxs1}\left(\Omega_{1x} - \omega_{1x}\right) + I_{xz1}\left(\Omega_{1z} - \omega_{1z}\right) - m_{R1}h_1 \cdot \left(V_{1y} - v_{1y}\right) - \\ m_{R1}h_1\frac{\Delta t}{2}\left(V_{1x}\Omega_{1z} + v_{1x}\omega_{1z}\right) = P_y\left(z_A - h_1\right) - D_{s1}\frac{\Delta t}{2}\left(\Omega_{1x} + \omega_{1x}\right) \end{aligned} \tag{10}$$

Two additional equations are derived from the coefficient of restitution (e) [10] and the coefficient of tangential interaction (μ) [11], both of which are assumed known a priori. They are defined below in Eq. (11) and Eq. (12).

$$e = -\frac{V_{2n} - V_{1n}}{v_{2n} - v_{1n}} \tag{11}$$

$$\mu = \frac{P_t}{P_n} = \frac{P_y\cos\Gamma - P_x\sin\Gamma}{P_x\cos\Gamma + P_y\sin\Gamma} \tag{12}$$

Finally, two more equations projects the collision impulses from the bullet vehicle coordinate frame to the target vehicle coordinate frame.

$$P_x = -P_{x'}\cos\theta_2 + P_{y'}\sin\theta_2\,,\; P_y = -P_{x'}\sin\theta_2 - P_{y'}\cos\theta_2 \tag{13}$$

These 12 equations can be collected and assembled in a matrix form that relates the post-impact vehicle states to the pre-impact states. Equation (14) presents the formulation in block matrix. The specific terms in matrix **A** and vector **B** are detailed in the Annex.

$$\begin{pmatrix} A_{11} & \mathbf{0} & A_{13} \\ \mathbf{0} & A_{22} & A_{23} \\ A_{31} & A_{32} & A_{33} \end{pmatrix} \cdot \mathbf{x} = \mathbf{B} \tag{14}$$

where $\mathbf{x} = \left(V_{1x} \;\; V_{1y} \;\; \Omega_{1z} \;\; \Omega_{1x} \;\; V_{2x'} \;\; V_{2y'} \;\; \Omega_{2z} \;\; \Omega_{2x'} \;\; P_x \;\; P_y \;\; P_{x'} \;\; P_{y'}\right)'$.

The unknown post-impact vehicle states and corresponding impulses can be resolved with an iterative approach. Finally, given the obtained impulses and the assumed collision time duration Δt, the impact force profile can be approximated.

Influences of Operating Variables and Parameters on a PIT Maneuver

The purpose of a PIT maneuver is to compel the target vehicle to "fishtail" so that the fleeing suspect cannot recover. One straightforward index of the severity of a PIT maneuver is the post-impact yaw rate of the pursued vehicle (Ω_{1z}). In this section, the models of pre-impact steering and vehicle collision developed in the two previous sections are applied to investigate the influences of operating variables (e.g., forward speed, initial lateral clearance, and steering wheel rate) and parameters (e.g., coefficient of restitution and road adhesion coefficient) on Ω_{1z}.

The parameters and operating conditions for the simulation are specified as follows. The two colliding vehicles are assumed to have the same vehicle parameters summarized in Tab. 1, which are extracted from the "big sedan" nonlinear model in CarSim software. In this section, unless otherwise specified, remaining essential parameters are fixed at their nominal values: forward speed (v_{1x} = 40 mph or 17.88 m/s), initial lateral clearance (ΔY = 0.8 m), steering wheel rate (k_δ = 260 deg/s), coefficient of restitution (e = 0.45), road adhesion coefficient (μ_R = 0.8), and coefficient of tangential interaction (μ = 0.12). Furthermore, the collision locations on vehicle bodies are assumed to be on the front fender (x_2 = 0.8 m ahead of the front axle) and the rear fender (x_1 = 0.9 m behind the rear axle).

TABLE 1. VEHICLE PARAMETERS ("BIG SEDAN" IN CARSIM)

Parameter	Value	Parameter	Value
a	1.033 (m)	h_{CG}	0.54 (m)
b	1.657 (m)	i_{SW}	16.0 : 1
C_f	137130 (N/rad)	I_{xxs}	850 (kg·m^2)
C_r	117670 (N/rad)	I_{xz}	20 (kg·m^2)
D_s	6500 (N·m·s/rad)	I_{zz}	3200 (kg·m^2)
K_s	70160 (N·m/rad)	m_{NR}	180 (kg)
h	0.40 (m)	m_R	1527 (kg)

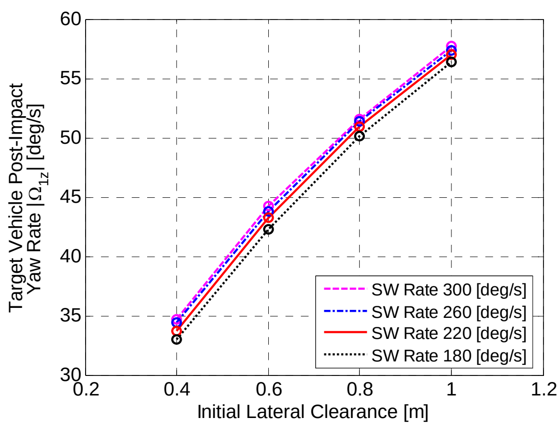

FIGURE 6. INFLUENCES OF INITIAL LATERAL CLEARANCE AND STEERING RATE ON PIT'S EFFECTIVENESS

Figure 6 shows the influences of the initial lateral clearance and the steering wheel rate on the post-impact yaw rate of the target vehicle, with four levels in each dimension. The figure indicates that other things being equal (e may decline with increasing relative velocity in actual situations), a realistically large initial lateral clearance is favorable for the PIT maneuver. The reason arises from the fact that given more lateral margin, the pursuer can develop a higher pre-impact yaw rate, and through the collision, more angular momentum will be transmitted to the target vehicle. Obviously, this initial lateral clearance has to be technically feasible to perform a PIT maneuver. In addition, a higher steering angular velocity leads to more effective results, but the benefits are marginal when the steering velocity is already sufficiently high.

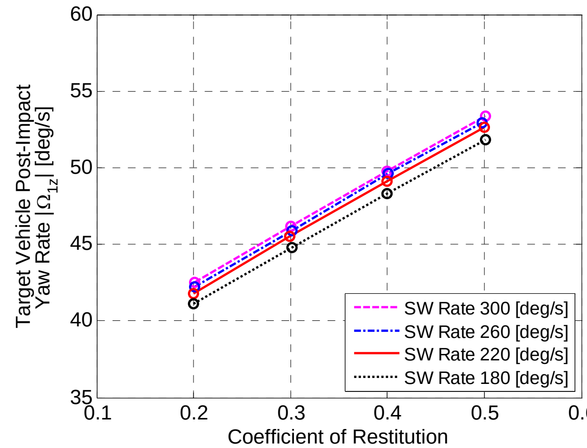

FIGURE 7. INFLUENCES OF COEFF. OF RESTITUTION AND STEERING RATE ON PIT'S EFFECTIVENESS

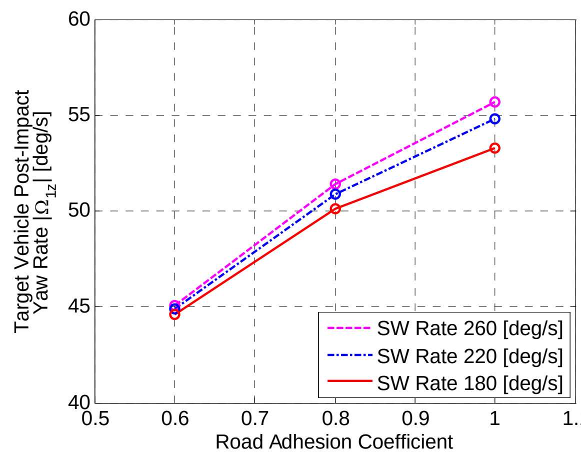

FIGURE 8. INFLUENCES OF ROAD ADHESION AND STEERING RATE ON PIT'S EFFECTIVENESS

The influences of the coefficient of restitution and the steering wheel rate on the post-impact yaw rate of the target are shown in Fig. 7. The coefficient of restitution has a strong influence on the PIT results: a higher restitution indicates less energy lost in the collision and more energy imparted to the target, hence more substantial post-impact yaw motions.

However, this is not a parameter that can be directly adjusted by the pursuer. It depends on body materials, surface geometry [12], relative velocities, among other factors. It is preferred that the striking area of the pursuing vehicle is composed of less deformable material and structure. In addition, the influence of road adhesion condition is illustrated in Fig. 8. Other things being equal, it is shown that roads with better adhesion conditions are conducive to the execution of a PIT maneuver.

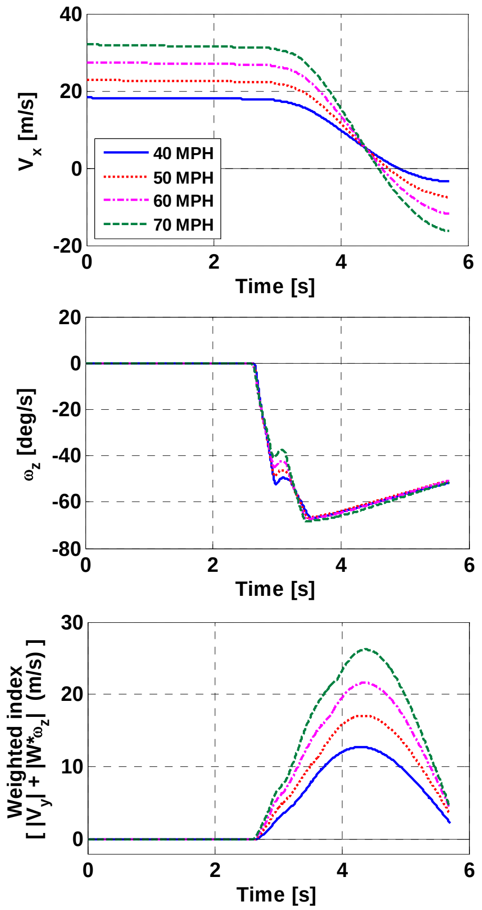

FIGURE 9. INFLUENCE OF VEHICLE VELOCITY ON PIT'S EFFECTIVENESS (TARGET VEHICLE'S RESPONSES)

Figure 9 presents the responses of the pursued vehicle at four different pre-impact velocities. Simulation settings are the same as outlined at the beginning of this section, except that the forward speed is chosen among 40, 50, 60, and 70 mph. The onset of collisions is approximately at 2.6 s, and no drivers' counter-steering is assumed for the post-PIT motions. In each scenario, two successive collisions occur before the two vehicles eventually separate from each other. At the end of the PIT maneuver, the peak post-impact yaw rates are fairly uniform across the four cases. However, it is incomplete to use yaw rate alone to characterize the vehicle because besides spinning, it is also skidding. A weighted index J is defined below as the sum of the absolute values of lateral velocity and a weighted yaw rate.

$$J = \left|v_y\right| + \left|W \times \omega_z\right| \tag{15}$$

The weight W is used to penalize instantaneous yaw rate and convert its unit into m/s. The choice of the weight is based on the steady-state cornering behavior of a linearized lateral/yaw vehicle model. It can be proven that the steady-state relationship between lateral velocity and yaw rate is a function of longitudinal velocity, if other parameters are fixed.

$$W\left(v_x\right) = \left.\frac{v_y}{\omega_z}\right|_{ss} = b - a\frac{Mv_x^2}{LC_r} \tag{16}$$

The bottom subplot in Fig. 9 shows that the disturbance by impact forces inflates the index J in all cases. At higher speeds, the combined effects of spinning and skidding after the maneuver is more pronounced. Although it destabilizes the pursued vehicle to a larger extent, it is more likely to induce unintended injuries since the pursued vehicle skids more at higher speeds. Because the ultimate purpose of PIT maneuver is to prevent the pursued from proceeding forward, instead of throwing it into complete instability, the execution of PIT maneuvers should be limited to relatively low speeds.

In brief, this section suggests guidelines to perform an effective PIT maneuver based on the analysis from the aspect of vehicle dynamics. It is demonstrated with simulations that a reasonably large lateral clearance and sufficiently fast pre-impact steering action are in favor of an effective PIT maneuver. In addition, the influences of road adhesion, the coefficient of restitution, as well as the forward speed are also revealed with numerical examples.

INTERACTION WITH STABILITY CONTROL SYSTEMS

After the pursued vehicle is subject to a PIT maneuver, the fleeing suspect may try very hard to regain directional control of the vehicle by counter-steering. In the meantime, active safety systems such as Electronic Stability Control (ESC) systems, if installed, may intervene to assist the driver to maintain control of the vehicle. The responses of the vehicle equipped with ESC can come as a surprise to the patrol police and make the PIT maneuver less effective.

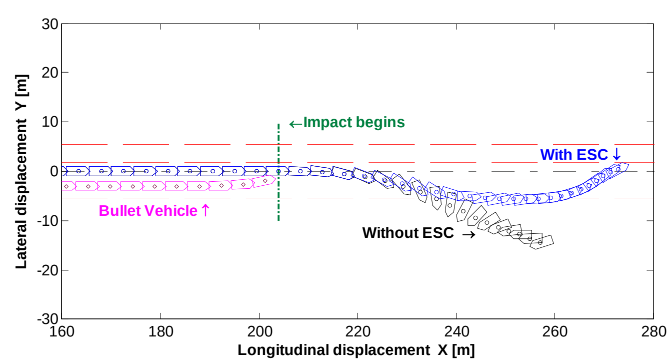

FIGURE 10. VEHICLE TRAJECTORIES IN A MILD PIT MANEUVER (WITH ESC VS. WITHOUT ESC)

Figure 10 illustrates the comparison of two otherwise identical vehicles subject to the same PIT collision disturbances, and their only difference is whether the ESC module is activated. The ESC algorithm is developed at Ford Motor Company for internal research purposes and well tuned for the vehicle simulated. Figure 10 depicts the trajectories of vehicles involved in the PIT at an initial travel speed of 50 mph (22.4 m/s). The responses of the pursued vehicles are contrasted in Fig. 11, along with ESC intervention braking pressures.

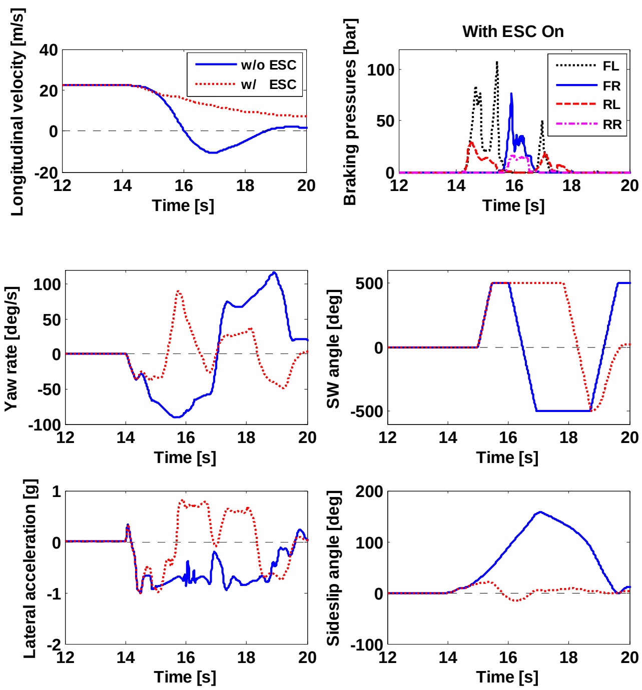

FIGURE 11. RESPONSES OF THE PURSUED VEHICLE IN A MILD PIT MANEUVER (WITH ESC VS. WITHOUT ESC)

It is evident that in Fig. 11, the ESC system begins to intervene promptly after the collision starts at 14 s, indicated by the braking pressures applied to the left side (top right subplot). With proper counter-steering by a skilled driver model (middle right subplot), the pursued vehicle with ESC "on" can attenuate the post-impact yaw rate and slip angle, and eventually proceeds in its original direction. In contrast, without the activation of the ESC, the driver model cannot recover from the collision. The vehicle develops substantial sideslip angle and spins out despite the driver's panic counter-steering efforts. Consequently, for the pursuing police, the prior knowledge of whether the fleeing vehicle is equipped with the ESC feature can better prepare the patrol sergeant for the possible outcome and to adjust the pursuing tactics.

For a more severe PIT maneuver (Fig. 12), even a skillful driver cannot stabilize the vehicle with the help of ESC. Both pursued vehicles develop substantial heading angles and practically spin out (responses are shown in Fig. 13). Since ESC is primarily designed to follow drivers' steering intention and to limit sideslip angles, but not for collision-induced motion attenuation, this limitation of effectiveness is expected. The threshold for the effectiveness of ESC against PIT, which relies on the design of ESC as well as the perturbed vehicle states, will be explored in future studies.

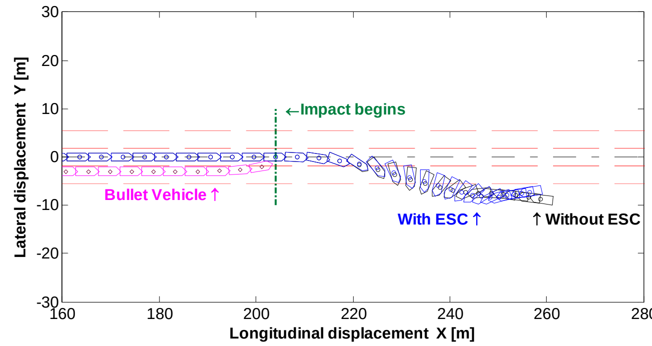

FIGURE 12. VEHICLE TRAJECTORIES IN A SEVERE PIT MANEUVER (WITH ESC VS. WITHOUT ESC)

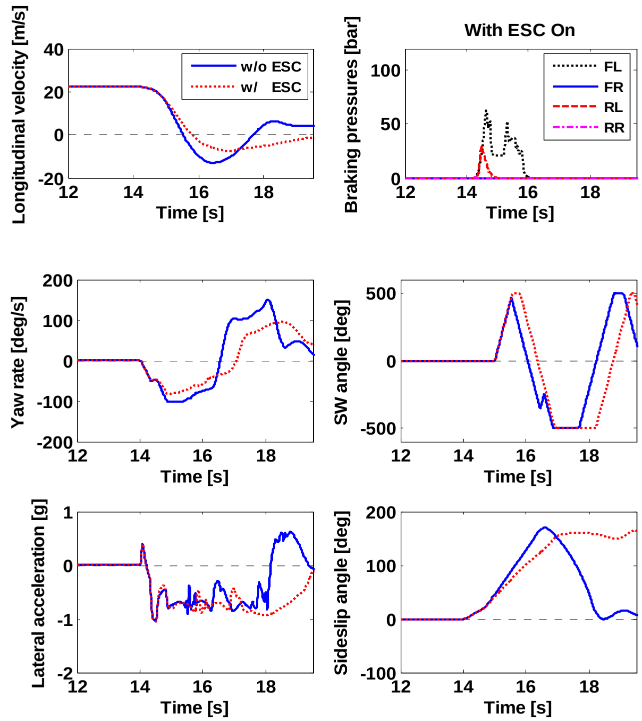

FIGURE 13. RESPONSES OF THE PURSUED VEHICLE IN A SEVERE PIT MANEUVER (WITH ESC VS. WITHOUT ESC)

CONCLUSIONS

In this work, we initiated an engineering analysis of the PIT maneuver, a pursuit-ending approach used by the law enforcement. This study concentrated on the mathematical modeling of the interaction between the vehicles involved in a PIT maneuver and the simulation of the loss-of-control of the pursued vehicle after the PIT maneuver. The influencing factors for the execution of the maneuver were explored. We also investigated the effectiveness of ESC systems equipped on modern vehicles in response to PIT. It is shown through simulations that the activation of ESC may help the driver recover after being hit by a mild PIT maneuver, but a severe PIT maneuver at a high speed can hardly be recovered by a skillful diver, even with the assistance of ESC. PIT involves high risks, especially at elevated speed. The authors do not endorse the use of PIT maneuver at high-speed situations. Only specially trained law enforcement officers should decide when to assume the risk of conducting PIT. These maneuvers should be conducted by professionals with special training.

In addition, a PIT maneuver performed against a vehicle with a high center of gravity may induce a rollover accident. A front-wheel-drive vehicle may respond differently from a rear-wheel-drive vehicle does, due to different tire force distribution patterns. These are parts of topics for future investigation.

ACKNOWLEDGMENTS

This work was supported by the Ford Motor Company. The authors thank the anonymous reviewers for helpful comments.

REFERENCES

[1] Ashley, S., 2002. “Reducing the Risks of Police Pursuit”. *Police and Security News*, 18(5), September/October.

[2] Eisenberg, C., 1999. “Pursuit Management”. *Law & Order*, 47(3), March, pp. 73–77.

[3] Daniels, W., 2002. “Low Cost Pursuit Intervention Training”. *Law & Order*, 50(6), June, pp. 24–26.

[4] “Hot Pursuit - Going For a Spin”. See URL http://www.trutv.com/video/index.html

[5] Peterson, C., 2006. “Why cops can't drive, Part 2”. *Law Officer Magazine*, April.

[6] Bayless, K.L. and Osborne, R., 1998. “Pursuit Management Task Force Report”. National Law Enforcement and Corrections Technology Center.

[7] Court case Scott v. Harris, No. 05–1631, U.S. Supreme Court, April 30 2007. See also URL http://www.supremecourtus.gov/opinions/06slipopinion.html

[8] Pinellas County Sheriff's Office (Florida), 2007. “Pursuit operation of sheriff's office vehicles”. General Order 15-2.

[9] Zhou, J., Peng, H., and Lu, J., 2007. “Collision Model for Vehicle Motion Prediction after Light Impacts”. Proc. 20th IAVSD Symposium, Berkeley, CA.

[10] Monson, K.L. and Germane, G.J., 1999. “Determination and Mechanisms of Motor Vehicle Structural Restitution from Crash Test Data”. SAE Paper 1999-01-0097.

[11] Marine, M.C., 2007. “On the Concept of Inter-Vehicle Friction and its Application in Automobile Accident Reconstruction”. SAE Paper 2007-01-0744.

[12] Cannon, J.W, 2001. “Dependence of a Coefficient of Restitution on Geometry for High Speed Vehicle Collisions”. SAE Paper 2001-01-0892.

ANNEX A

ENTRIES FOR THE MATRIX IN EQ. (14)

$$A_{11} = \begin{pmatrix} m_1 & 0 & -m_1 \frac{\Delta t}{2} V_{1y} & 0 \\ 0 & m_1 + \frac{\Delta t}{2} \frac{C_{f1} + C_{r1}}{V_{1x}} & m_1 \frac{\Delta t}{2} V_{1x} + \frac{\Delta t}{2} \frac{a_1 C_{f1} - b_1 C_{r1}}{V_{1x}} & -m_{R1} h_1 \\ 0 & \frac{\Delta t}{2} \cdot \frac{-a_1 C_f + b_1 C_r}{V_{1x}} & -I_{zz1} - \frac{\Delta t}{2} \frac{a_1^2 C_{f1} + b_1^2 C_{r1}}{V_{1x}} & -I_{xz1} \\ 0 & -m_{R1} h_1 & I_{xz1} - m_{R1} h_1 \frac{\Delta t}{2} V_{1x} & I_{xxs1} + \frac{\Delta t}{2} D_{s1} \end{pmatrix}, \quad A_{13} = \begin{pmatrix} -1 & 0 & 0 & 0 \\ 0 & -1 & 0 & 0 \\ -y_A & x_A & 0 & 0 \\ 0 & -(z_A - h_1) & 0 & 0 \end{pmatrix}$$

$$A_{22} = \begin{pmatrix} m_2 & 0 & -m_2 \frac{\Delta t}{2} V_{2y'} & 0 \\ 0 & m_2 + \frac{\Delta t}{2} \frac{C_{f2} + C_{r2}}{V_{2x'}} & m_2 \frac{\Delta t}{2} V_{2x'} + \frac{\Delta t}{2} \frac{a_2 C_{f2} - b_2 C_{r2}}{V_{2x'}} & -m_{R2} h_2 \\ 0 & \frac{\Delta t}{2} \cdot \frac{-a_2 C_{f2} + b_2 C_{r2}}{V_{2x'}} & -I_{zz2} - \frac{\Delta t}{2} \frac{a_2^2 C_{f2} + b_2^2 C_{r2}}{V_{2x'}} & -I_{xz2} \\ 0 & -m_{R2} h_2 & I_{xz2} - m_{R2} h_2 \frac{\Delta t}{2} V_{2x'} & I_{xxs2} + \frac{\Delta t}{2} D_{s2} \end{pmatrix}, A_{23} = \begin{pmatrix} 0 & 0 & -1 & 0 \\ 0 & 0 & 0 & -1 \\ 0 & 0 & -y_{A'} & x_{A'} \\ 0 & 0 & 0 & -(z_{A'} - h_2) \end{pmatrix}, \quad A_{31} = \begin{pmatrix} 0 & 0 & 0 & 0 \\ 0 & 0 & 0 & 0 \\ 0 & 0 & 0 & 0 \\ \cos\Gamma & \sin\Gamma & d_c \cos\Gamma - d_d \sin\Gamma & 0 \end{pmatrix}$$

$$A_{32} = \begin{pmatrix} 0 & 0 & 0 & 0 \\ 0 & 0 & 0 & 0 \\ 0 & 0 & 0 & 0 \\ -\sin\theta_2 \sin\Gamma - \cos\theta_2 \cos\Gamma & \sin\theta_2 \cos\Gamma - \cos\theta_2 \sin\Gamma & d_a \cos\Gamma - d_b \sin\Gamma & 0 \end{pmatrix}, \quad A_{33} = \begin{pmatrix} 1 & 0 & \cos\theta_2 & -\sin\theta_2 \\ 0 & 1 & \sin\theta_2 & \cos\theta_2 \\ \mu\cos\Gamma + \sin\Gamma & \mu\sin\Gamma - \cos\Gamma & 0 & 0 \\ 0 & 0 & 0 & 0 \end{pmatrix}$$

$\mathbf{B} = \begin{pmatrix} m_1 v_{1x} & 0 & 0 & 0 & m_2 v_{2x'} & 0 & 0 & 0 & 0 & 0 & 0 & B_{12} \end{pmatrix}'$, where $B_{12} = -e\left[(-v_{2x'} \sin\theta_2) \cdot \sin\Gamma + (v_{1x} - v_{2x'} \cos\theta_2) \cdot \cos\Gamma\right]$